Arch. Metall. Mater. **63** (2018), 3, 1217-1224

DOI: 10.24425/123794

X. FU*#, M. CHU*, L. GAO*, Z. LIU*

MECHANISM AND KINETICS STUDIES ON NON-ISOTHERMAL DECOMPOSITION OF LUDWIGITE IN INERT ATMOSPHERE

Ludwigite is the main available boron-bearing resource in China. In order to enrich the theory system and optimize its utilization processes, this paper study the mechanism and kinetics on non-isothermal decomposition of ludwigite in inert atmosphere by means of thermal analysis. Results show that, the decomposition of serpentine and szajbelyite is the main cause of mass loss in the process. At the end of decomposition, hortonolite and ludwigite are the two main phases in the sample. The average E value of structural water decomposition is 277.97 kJ/mol based on FWO method (277.17 kJ/mol based on KAS method). The results is proved to be accurate and reliable. The mechanism model function of structural water decomposition is confirmed by Satava method and Popescu method. The form of the most probable model function is $G(\alpha) = (1 - \alpha)^{-1} - 1$ (integral form) and $f(\alpha) = (1 - \alpha)^2$ (differential form), and its mechanism is chemical reaction. This is verified by the criterion based on activation energy of model-free kinetics analysis.

Keywords: ludwigite; non-isothermal decomposition; kinetics; activation energy; model function

1. Introduction

As an important chemical material, boron and its compounds play essential roles in many aspects of modern science and technology field. With the steady and fast development of China's economy, the market demand of boron products is increasing sharply [1-2]. However, the current supply of boron resources cannot meet the demand of chemical industry. Therefore, it is vital to find effective processes for developing and utilizing complex boron ore resources.

Boron ores mainly consist of ascharite and ludwigite in China. Recently, the ascharite is nearly exhausted; thus, as a large-scale boron ore deposit with high-utility value of valuable elements, ludwigite ore in northeastern China has been a hot issue among researchers [3-5]. In the past decades, trial utilization routes of ludwigite mainly include pyrometallurgical process [6-11] and hydrometallurgical process [12-17]. In the variable processes, especially the pyrometallurgical process, the thermal decomposition characteristics of ludwigite is an important factor for selecting or improving the reasonable thermal treatments to optimize production process and lessen energy consumption. This paper analyze the mechanism and kinetics of thermal decomposition in inert atmosphere for ludwigite by means of thermal analysis method in details, in order to optimize the theoretical system for the efficient utilization of the valuable resource.

2. Experiments

2.1. Materials and methods

The main chemical compositions of ludwigite original ore from Dandong region is shown in Table 1 and its main patterns are shown in Fig. 1. Serpentine and szajbelyite are two main phases containing structural water, which can decompose when heated to high temperature as Eq. (1) and Eq. (2) describe. Based on the HSC Chemistry, the standard Gibbs free energy of Eq. (1) can be presented as $\Delta G^{\theta} = 198.30\text{-}0.30T$ (kJ/mol). For Eq. (2), unfortunately, the standard Gibbs free energy cannot be presented here because no authoritative thermodynamic data of szajbelyite has been published up to now.

TABLE 1

The main chemical composition of ludwigite original ore

Component	TFe	FeO	Fe_2O_3	B_2O_3	MgO	SiO_2	CaO	Al_2O_3
Content/%	30.66	17.57	24.28	8.61	26.42	14.30	0.19	0.89

$$2(Mg,Fe)_3Si_2O_5(OH)_4(s) = 3(Mg,Fe)_2SiO_4(s) + \\ + SiO_2(s) + 4H_2O(g) \quad (1)$$

$$2MgBO_2(OH)(s) = Mg_2B_2O_5\,(s) + H_2O(g) \quad (2)$$

* NORTHEASTERN UNIVERSITY, SCHOOL OF METALLURGY, NO. 3-11, WENHUA ROAD, HEPING DISTRICT, SHENYANG, P. R. CHINA, 110819 SHENYANG, CHINA

Corresponding author: fxj.2046@163.com

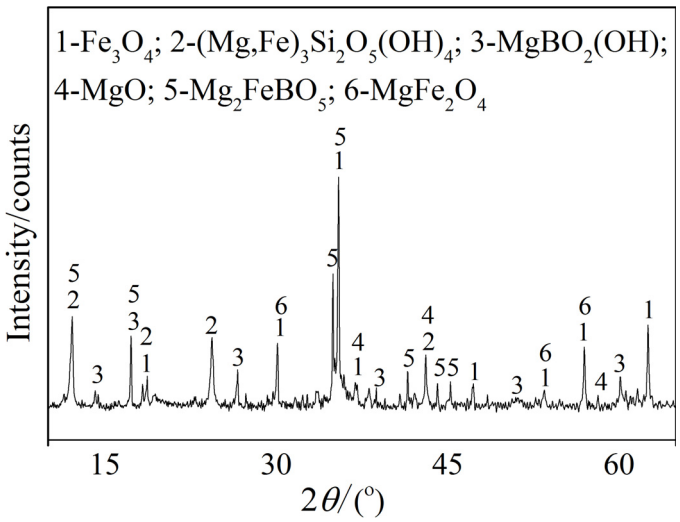

Fig. 1. XRD analysis of ludwigite original ore

The experiments of non-isothermal decomposition for ludwigite were carried out using a Netzsch STA409 C/CD analyzer, and the procedure was described as follows: firstly, the ludwigite original ore was ground to particle size less than 0.074 mm; then, a sample of about 8 mg was injected into an alumina crucible for each run and heated from room temperature to 1273 K under a steady Ar flow(99.99%, volume fraction) of 40 mL/min, and the heating rates were 5 K/min, 10 K/min, 20 K/min, respectively; finally, the original data was collected for follow-up research on mechanism and kinetics of non-isothermal decomposition for ludwigite in inert atmosphere.

2.2. Kinetics analysis methods

In general, the rate of the decomposition of the non-isothermal and heterogeneous reaction can be expressed as a function of conversion degree α and temperature T as shown in Eq. (3) [18-20],

$$\mathrm{d}\alpha/\mathrm{d}T = (1/\beta)\, k(T) f(\alpha) \tag{3}$$

Where, β is the linear heating rate, K/min; α is the conversion degree which can be defined by Eq. (4); $k(T)$ is the temperature dependency which can be described by the Arrhenius expression Eq. (5); $f(\alpha)$ is the kinetic model function,

$$\alpha = (m_i - m_T)/(m_i - m_f) \tag{4}$$

Where, m_i is the initial mass of the sample during the specified thermal decomposition stage; m_T is the mass of the sample residue at temperature T; m_f is the final mass of the sample during the specified thermal decomposition stage.

$$k(T) = A \exp(-E/RT) \tag{5}$$

Where, A is the pre-exponential factor, R is the gas constant and E is the activation energy. Eq. (6) can be obtained by substituting Eq. (5) in Eq. (3) and integrating by separation of variables,

$$G(\alpha) = \int_0^{\alpha} \mathrm{d}\alpha / f(\alpha) = \int_0^{T} \exp(-E/RT)\,\mathrm{d}T = (AE/\beta R)\, E/RT \tag{6}$$

Where, $G(\alpha)$ is the integral form of $f(\alpha)$; E/RT is generally defined as a temperature integral, which has different expressions with different mathematical analytical methods [18].

Two different isoconversional free-model methods, namely Flynn-Wall-Ozawa (FWO) method and Kissinger-Akahira-Sunoe (KAS) method, are used to analyze the activation energy of the thermal decomposition as a function of conversion [18,21-23]. The FWO and KAS method are expressed in Eq. (7) and Eq. (8), respectively,

$$\lg\beta = \lg(AE/RG(\alpha)) - 2.315 - 0.4567E/RT \tag{7}$$

$$\ln(\beta/T^2) = \ln(AR/EG(\alpha)) - E/RT \tag{8}$$

According to the above two free-model kinetic methods, with a series of different heating rates, the activation energy of the specific value of α can be calculated from the slopes of fitting line $\lg\beta - 1/T$ and $\ln(\beta/T^2) - 1/T$, respectively. The activation energy value E_o obtained by FWO can be used for validating the correctness of kinetic model function calculated by other kinetic methods.

Two different kinetic model function methods, namely Satava method(single heating rate method) and Popescu method(multi-heating rate method), are used for solving the most probable model function during the decomposition process of phases containing structural water. Satava method is expressed in Eq. (9) [18,24],

$$\lg[G(\alpha)] = \lg(AE/\beta R) - 2.315 - 0.4567E/RT \tag{9}$$

For the correct $G(\alpha)$, the curve of $\lg[G(\alpha)]$ to $1/T$ must be a straight line. If only one $G(\alpha)$ satisfies the linear relationship, this $G(\alpha)$ is the most probable model function. If more than one $G(\alpha)$ satisfy the linear relationship, the $G(\alpha)$ with the calculated activation energy $E_s \approx E_o\left(|E_s - E_o|/E_o \le 0.1\right)$ is chosen as the most probable model function.

For the Popescu method [18,25,26], the corresponding conversion degree (α_{mi}, α_{ni}) at T_m and T_n can be determined from the experimental data, so as the corresponding conversion degree (T_{mi}, T_{ni}) at α_m and α_n. Eq. (10) can be obtained by definite integration Eq. (3) of both sides,

$$\int_{\alpha_m}^{\alpha_n} d\alpha / f(\alpha) = 1/\beta \int_{T_m}^{T_n} k(T)\, dT \tag{10}$$

By definition the left side and right side of Eq. (10) as Eq. (11) and Eq. (12) respectively, Eq. (10) can be rewritten as Eq. (13),

$$G(\alpha)_{mn} = \int_{\alpha_m}^{\alpha_n} d\alpha / f(\alpha) \tag{11}$$

$$I(T)_{mn} = \int_{T_m}^{T_n} k(T)\,dT \tag{12}$$

$$G(\alpha)_{mn} = 1/\beta \cdot I(T)_{mn} \tag{13}$$

For the reasonable range of α and β, the forms of $k(T)$ and $f(\alpha)$ do not change, the relationship of $G(\alpha)_{mn}$ to $1/\beta_i$ must be a line with the coordinates (0,0) on it. If the experimental data and the adopted $G(\alpha)$ meet the above relationship, this $G(\alpha)$ must be the most probable model function. The activation energy E and pre-exponential factor A are calculated by Eq. (14), where, $T_a = (T_n + T_m)/2$,

$$\ln[\beta/(T_n - T_m)] = \ln[A/G(\alpha)] - E/RT_a \tag{14}$$

Neither any approximate forms of temperature integral nor concrete form of $k(T)$ is introduced when solved the most probable model function by Popescu method. The obvious advantage makes the results more reliable by this method.

3. Results and discussions

3.1. Non-isothermal analysis of ludwigite

Based on the original weight loss data collected from thermal analyzer, the conversion degree α is calculated by Eq. (4), and the reaction rate $d\alpha/dT$ is the first derivative of conversion degree versus temperature. The results are shown in Fig. 2. The $d\alpha/dT$ curve in Fig. 2 has three obvious peaks, which indicate the whole decomposition process can be divided into three stages. The first peak mainly represent the removal of the absorb water in the sample at the low temperature range from room temperature to about 450 K. The second peak mainly represent the removal of the crystal water and/or some interlayer water in the sample at the medium temperature range about from 450 K to 700 K. The third peak with temperature above 800 K represents the decomposition of the two main phases containing structural water, namely serpentine and szaibelyite. It is the main decomposition reaction of ludwigite when heated in inert atmosphere, and its reaction rate is fast and mass loss is evident. The single, evident, sharp and narrow peak above 800K at $d\alpha/dT$ curve indicates the decomposition temperature of serpentine and szaibelyite in the ludwigite original ore is very close under this research conditions. Under different heating rates, $\alpha - d\alpha/dT$ plots present the similar distribution status with three main peaks as temperature increases. The curves at quick heating rate lag behind the curves at slow heating rate, and it indicates with the heating rate increasing, the decomposition temperature of ludwigite rises at some extent. The corresponding top temperatures of each peak at different heating rates are: Peak 1, 376.85 K, 404.07 K, 428.39 K; Peak 2, 656.73 K, 670.29 K, 682.52 K; Peak 3, 890.02 K, 909.39 K, 921.04 K; respectively.

3.2. XRD analysis of thermal decomposition of ludwigite

Phase analysis of ludwigite at different temperatures during the thermal decomposition process are shown in Fig. 3. At the temperature of 750 K, magnetite and ludwigite are the two

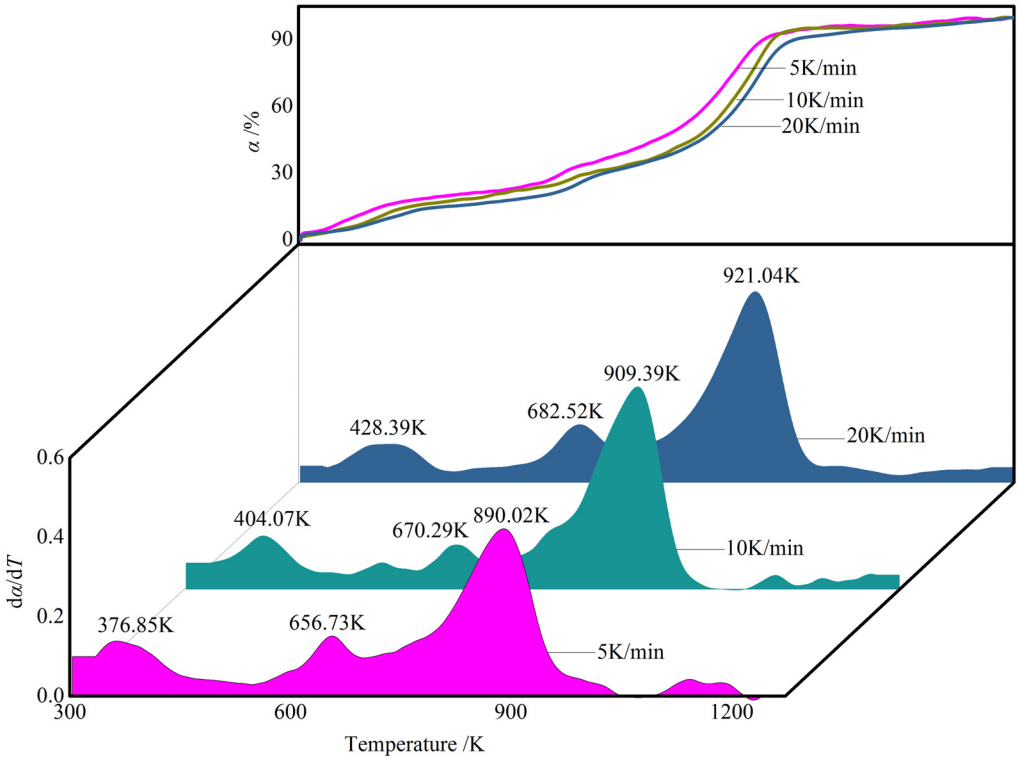

Fig. 2. $\alpha - d\alpha/dT$ for the thermal decomposition of ludwigite at different heating rates

main phases in the sample, accompanied by serpentine whose diffraction peaks weaken at some extent, and diffraction peaks of szaibelyite are not evident any more. It is on one hand because szaibelyite decomposes at a certain amount at the temperature, on the other hand because the removal of interlayer water may affect the crystallinity degree of the phases, especially those containing hydroxy. At the temperature of 900 K, most of serpentine has decomposed and generate hortonolite. In addition, suanite is not discovered in the sample, and the diffraction peaks of ludwigite enhance to some extent, which indicates the decomposition product of szaibelyite reproduce new ludwigite combined with magnetite or pleonaste. At the temperature of 1050 K, the sample has no or few hematite, and ferric iron exists largely in ludwigite and pleonaste. During the non-isothermal decomposition process of ludwigite ore, original phases decompose and transform accompanied with the combination and generation of new phases. At the temperature of 1200 K, hortonolite and ludwigite are the two main phases in the sample. In summary, the phase changes of elements during non-isothermal decomposition can be described as Fig. 3b.

3.3 Model-free kinetics analysis on structural water decomposition

From the above analysis, phases containing structural water decomposition is the main reaction and energy consumption period during the whole decomposition of ludwigite. For further study, this paper carries out the kinetics calculations on structural water decomposition in the sample by different methods. The corresponding conversion degree α at the designated T and the corresponding T of the designated α at different heating rate β in the stage are shown in Table 2.

Substituting the data into Eq. (7) and Eq. (8) according to FWO and KAS, the fitting lines can be plotted and the activation energy E can be calculated from the line slopes. The results are shown in Fig. 4. The correlation coefficient R and the activation energy E based on model-free kinetics are summarized into Table 3. As shown, all the points exhibit a good correlation

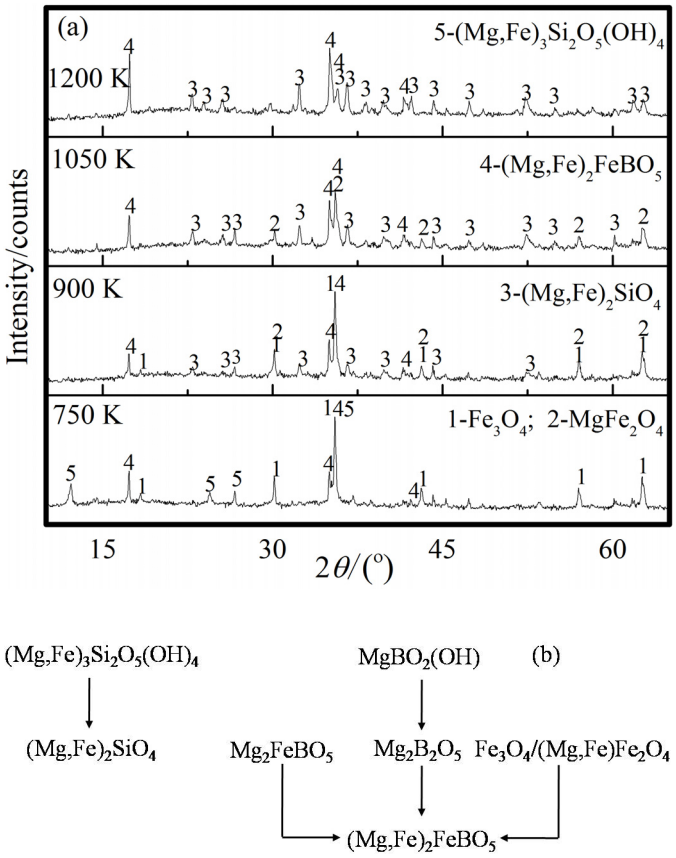

Fig. 3. Phase analysis of ludwigite during thermal decomposition process-(a)

coefficient for both FWO and KAS methods. Both methods present the similar trend for the distribution of the E values with the changed α, and it proves the accuracy and reliability of the calculated results. With the conversion degree increasing less than 0.7, the activation energy demonstrates an increase tendency. The average E value of this period is 277.97 kJ/mol based on FWO method (277.17 kJ/mol based on KAS method). Generally, the decomposition of structural water needs break the

TABLE 2

The corresponding α at the designated T and the corresponding T of the designated α at different heating rate β in structural water decomposition period

Designated T/K	Corresponding α at different β/–			Designated α/–	Corresponding T at different β/K		
	5 K/min	10 K/min	20 K/min		5 K/min	10 K/min	20 K/min
873.15	0.267	0.097	0.012	0.200	865.44	885.38	898.89
883.15	0.363	0.181	0.077	0.250	871.25	890.97	904.53
893.15	0.457	0.270	0.152	0.300	876.63	896.37	909.92
903.15	0.558	0.365	0.238	0.350	881.81	901.60	915.00
913.15	0.649	0.468	0.331	0.400	887.03	906.62	919.83
923.15	0.726	0.578	0.435	0.450	892.43	911.48	924.53
				0.500	897.47	916.18	929.17
				0.550	902.39	920.68	933.91
				0.600	907.54	925.06	938.93
				0.650	913.25	929.41	944.51
				0.700	919.47	933.94	951.17
				0.750	926.99	938.89	960.29

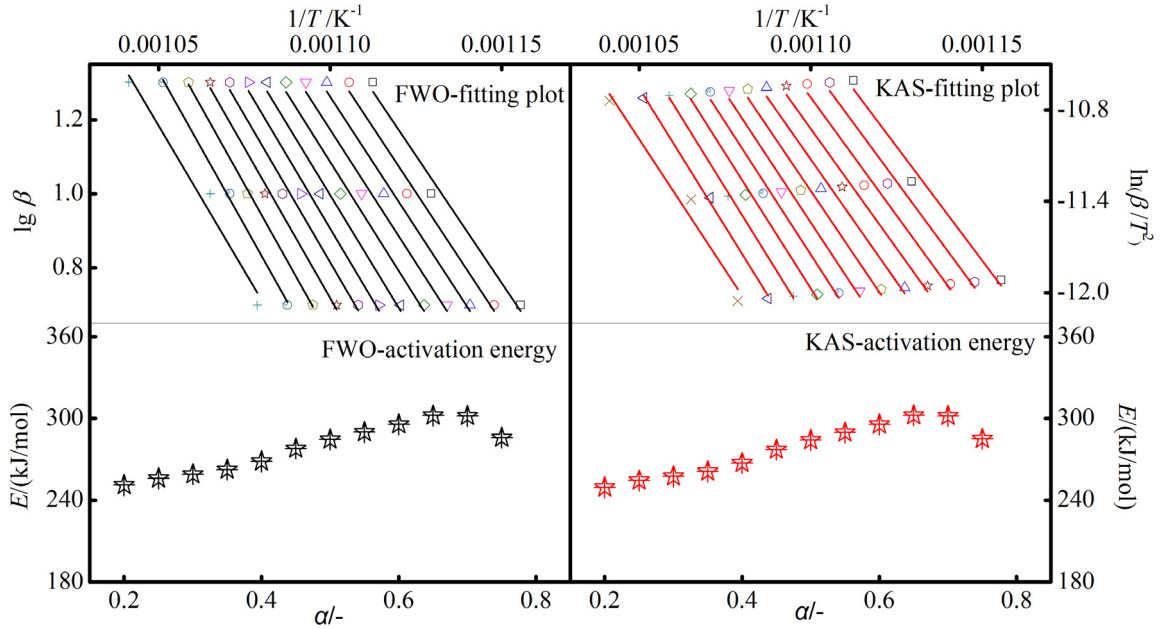

Fig. 4. The linear fitting plots and calculated E based on FWO and KAS methods of structural water decomposition

TABLE 3

The summarized results of structural water decomposition based on FWO and KAS

α/–	FWO		KAS	
	R/–	E/(kJ/mol)	R/–	E/(kJ/mol)
0.200	0.971	251.17	0.968	249.47
0.250	0.973	256.03	0.970	254.52
0.300	0.973	259.02	0.970	257.55
0.350	0.971	262.56	0.968	261.17
0.400	0.970	268.53	0.967	267.38
0.450	0.973	277.90	0.970	277.14
0.500	0.974	284.64	0.972	284.15
0.550	0.979	290.02	0.977	289.72
0.600	0.988	295.75	0.987	295.67
0.650	0.998	302.19	0.998	302.34
0.700	0.997	301.84	0.996	301.86
0.750	0.953	286.01	0.947	285.07
Average	0.974	277.97	0.974	277.17

chemical bonds in the original ore and form new compounds with residual atoms, and the energy needed in the process is much higher than the removal of non-structural water in the ore. Besides, it is another cause of the relatively high average activation energy that two main phases containing structural water (serpentine and szaibelyite) decompose at very similar temperature range.

3.4. Kinetics model functions analysis on structural water decomposition

For further study, this section analyzes the kinetics model functions on structural water decomposition in the sample by Satava method and Popescu method verified by FWO results. For each fixed β and 30 probable kinds of kinetics model functions of decomposition process[18], the fitting plots can be obtained by substituting the matching data in Table 3 into Eq. (9) by Satava method. It indicates 16 kinds of functions satisfy the best linear relationship ($R \geq 0.99$). The fitting results are shown in Fig. 5 and the functions forms and calculated activation energy are shown in Table 4. As can be seen, although there are 16 kinds of functions exhibiting good linear fitting results, only Function 29 meet the criterion based on activation energy ($|E_s - E_o|/E_o = 0.001 \leq 0.1$). It demonstrates Function 29 would likely be the most probable model function for the structural water decomposition in ludwigite, the mechanism of which is chemical reaction and the function form is $G(\alpha) = (1-\alpha)^{-1} - 1$ (integral form) and $f(\alpha) = (1-\alpha)^2$ (differential form).

For further confirmation on the most probable mechanism model function for the structural water decomposition process, this paper adopt Popescu method analyzing the above 16 kinds of probable functions further. Based on Table 4 and Eq. (10)~(13), the analyzed results with the coordinates (0,0) on the fitting plots are shown in Fig. 6 and Table 5. The correlation coefficient R reflect the goodness of fitting results, and the standard deviations SD stand for the variation size between actual value and the return value of linear, which is expected as small as possible. Taking R and SD into account, the most probable model function would be ensured. From Table 5, Function 29 is the best one with both greater R and smaller SD, and its function form is $G(\alpha) = (1-\alpha)^{-1} - 1$ (integral form) and $f(\alpha) = (1-\alpha)^2$ (differential form). Popescu method (multi-heating rate method) and Satava method (single heating rate method) indicate an excellent agreement on the most probable model function for the structural water decomposition process, and it proves the accuracy and reliability of the analyzed kinetics results.

Based on the obtained most probable model function, by substituting the matching data in Table 2 into Eq. (14) and plot-

TABLE 4

16 kinds of probable functions forms and calculated activation energy by Satava method

Function	$G(\alpha)$	$f(\alpha)$	E_s	$\lvert(E_s - E_o)/E_o\rvert$
3	$(1 - 2\alpha/3) - (1 - \alpha)^{2/3}$	$3[(1 - \alpha)^{-1/3} - 1]^{-1}/2$	341.14	0.227
4	$[1 - (1 - \alpha)^{1/3}]^2$	$3(1 - \alpha)^{2/3}[1 - (1 - \alpha)^{1/3}]^{-1}/2$	367.63	0.323
5	$[1 - (1 - \alpha)^{1/3}]^{1/2}$	$3(1 - \alpha)^{2/3}[1 - (1 - \alpha)^{1/3}]^{1/2}/(1/2)$	91.91	0.669
6	$[1 - (1 - \alpha)^{1/2}]^{1/2}$	$4(1 - \alpha)^{1/2}[1 - (1 - \alpha)^{1/2}]^{1/2}$	87.03	0.687
9	$-\ln(1 - \alpha)$	$(1 - \alpha)$	204.67	0.264
10	$[-\ln(1 - \alpha)]^{2/3}$	$3(1 - \alpha)\,[-\ln(1 - \alpha)]^{1/3}/2$	136.45	0.509
11	$[-\ln(1 - \alpha)]^{1/2}$	$2(1 - \alpha)\,[-\ln(1 - \alpha)]^{1/2}$	102.34	0.632
12	$[-\ln(1 - \alpha)]^{1/3}$	$3(1 - \alpha)\,[-\ln(1 - \alpha)]^{2/3}$	68.23	0.755
13	$[-\ln(1 - \alpha)]^4$	$(1 - \alpha)\,[-\ln(1 - \alpha)]^{-3}/4$	818.70	1.945
14	$[-\ln(1 - \alpha)]^{1/4}$	$4(1 - \alpha)\,[-\ln(1 - \alpha)]^{3/4}$	51.17	0.816
15	$[-\ln(1 - \alpha)]^2$	$(1 - \alpha)\,[-\ln(1 - \alpha)]^{-1}/2$	409.35	0.473
16	$[-\ln(1 - \alpha)]^3$	$(1 - \alpha)\,[-\ln(1 - \alpha)]^{-2}/3$	614.03	1.209
17	$1 - (1 - \alpha)^{1/2}$	$2(1 - \alpha)^{1/2}$	174.06	0.374
21	$1 - (1 - \alpha)^{1/3}$	$3(1 - \alpha)^{2/3}$	183.81	0.339
22	$1 - (1 - \alpha)^{1/4}$	$4(1 - \alpha)^{3/4}$	188.86	0.321
29	$(1 - \alpha)^{-1} - 1$	$(1 - \alpha)^2$	278.12	0.001

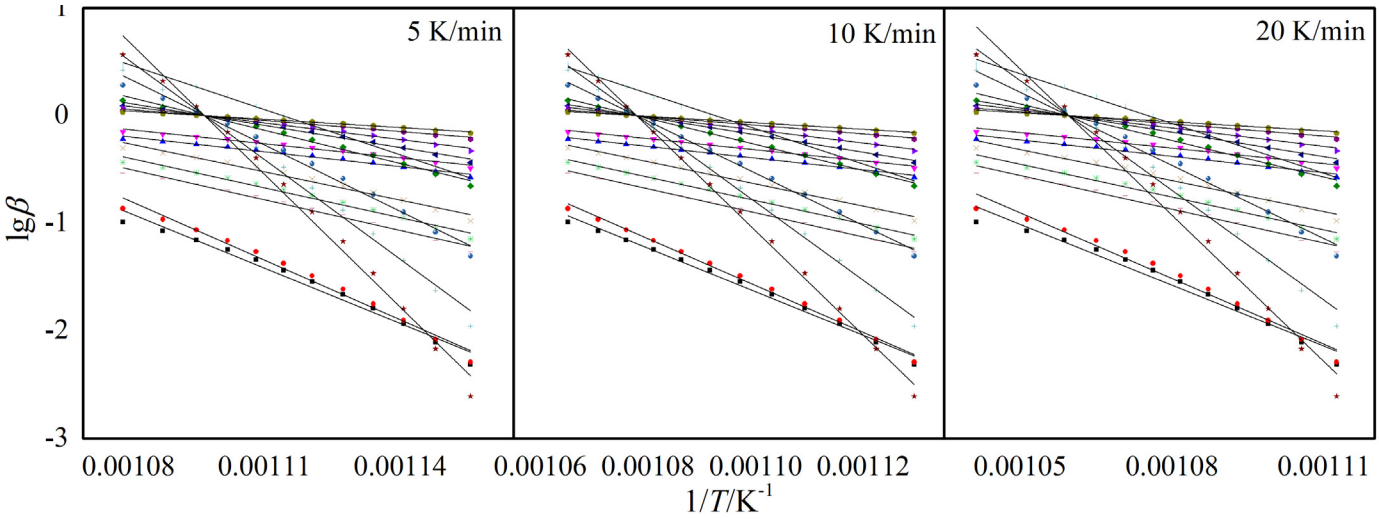

Fig. 5. 16 kinds of probable functions fitting plots by Satava method

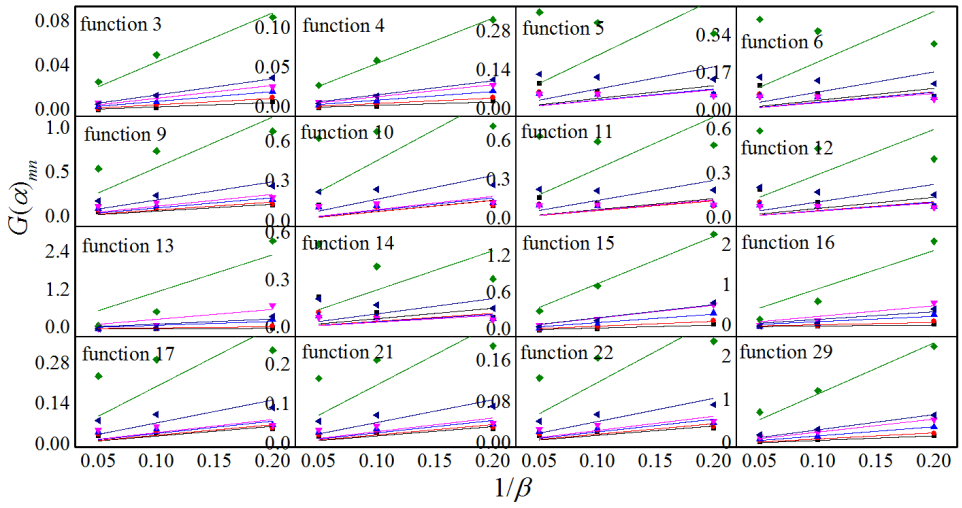

Fig. 6. 16 kinds of probable functions fitting plots by Popescu method

TABLE 5

Analyzed results of 16 kinds of probable functions by Popescu method

Function		3	4	5	6	9	10	11	12
R	T_m = 873.15K	0.937	0.925	0.390	0.367	0.936	0.560	0.438	0.214
SD	T_n = 883.15K	0.000	0.000	0.008	0.011	0.001	0.011	0.022	0.033
R	T_m = 883.15K	0.990	0.980	0.551	0.522	0.913	0.732	0.607	0.471
SD	T_n = 893.15K	0.000	0.000	0.004	0.005	0.003	0.008	0.011	0.011
R	T_m = 893.15K	0.999	0.994	0.634	0.600	0.925	0.791	0.699	0.595
SD	T_n = 903.15K	0.000	0.000	0.003	0.004	0.004	0.008	0.008	0.007
R	T_m = 903.15K	0.985	0.998	0.613	0.573	0.894	0.769	0.691	0.605
SD	T_n = 913.15K	0.000	0.000	0.003	0.004	0.007	0.010	0.009	0.006
R	T_m = 873.15K	0.989	0.998	0.539	0.504	0.890	0.730	0.610	0.464
SD	T_n = 923.15K	0.000	0.000	0.093	0.136	0.136	0.254	0.293	0.274
R	T_m = 883.15K	0.998	0.989	0.593	0.561	0.920	0.764	0.654	0.532
SD	T_n = 903.15K	0.000	0.000	0.012	0.018	0.013	0.031	0.037	0.034
Function		**13**	**14**	**15**	**16**	**17**	**21**	**22**	**29**
R	T_m = 873.15K	0.694	0.112	0.904	0.762	0.888	0.906	0.914	0.990
SD	T_n = 883.15K	0.000	0.034	0.001	0.001	0.000	0.000	0.000	0.000
R	T_m = 883.15K	0.737	0.401	0.961	0.825	0.845	0.870	0.881	0.988
SD	T_n = 893.15K	0.002	0.009	0.001	0.002	0.001	0.000	0.000	0.001
R	T_m = 893.15K	0.764	0.541	0.974	0.856	0.846	0.875	0.889	0.995
SD	T_n = 903.15K	0.015	0.005	0.002	0.010	0.001	0.000	0.000	0.001
R	T_m = 903.15K	0.808	0.560	0.995	0.904	0.782	0.823	0.842	0.996
SD	T_n = 913.15K	0.076	0.004	0.001	0.025	0.002	0.001	0.001	0.000
R	T_m = 873.15K	0.850	0.384	0.997	0.930	0.799	0.832	0.847	0.992
SD	T_n = 923.15K	0.816	0.228	0.006	0.235	0.035	0.016	0.009	0.041
R	T_m = 883.15K	0.757	0.467	0.970	0.847	0.846	0.873	0.886	0.993
SD	T_n = 903.15K	0.026	0.027	0.005	0.022	0.004	0.002	0.001	0.003

ting fitting lines of $\ln[\beta/(T_n - T_m)]$ vs $1/T_a$, the activation energy E_p and pre-exponential factor A can be calculated from the fitting line slope and intercept. The results are shown in Table 6. As can be seen, the activation energy E_p is 287.54 kJ/mol, the pre-exponential factor $\lg A$ is 15.69 s^{-1}, and the correlation coefficient R is 0.966. The result meet the criterion based on activation energy $(|E_p - E_o|/E_o = 0.03 \leq 0.1)$, and it further proves the correctness of the most probable model function of structural water decomposition process.

TABLE 6

Kinetics parameters values calculated by Popescu method

(α_m, α_n)	R/–	E/(kJ·mol^{-1})	$\lg A$/(s^{-1})
(0.2, 0.75)	0.966	287.54	15.69
(0.25, 0.75)	0.959	289.33	15.79
(0.3, 0.75)	0.950	290.71	15.88

4. Conclusions

(1) During the non-isothermal decomposition process in inert atmosphere, the decomposition of serpentine and szaibelyite is the main reaction in the process. At the decomposition end, hortonolite and ludwigite are the two main phases in the sample.

(2) Based on free-model kinetics analysis, the activation energy of structural water decomposition process of ludwigite is calculated by two different isoconversional methods FWO and KAS. The average E value of structural water decomposition is 277.97 kJ/mol based on FWO method (277.17 kJ/mol based on KAS method). Two methods indicate an excellent agreement on the distribution of E as changed α with an insignificant difference in the E values, and it proves the accuracy and reliability of the analyzed kinetics of ludwigite thermal decomposition process.

(3) The mechanism model function of structural water decomposition in ludwigite is confirmed by two methods, namely Satava method and Popescu method. Both methods indicate an excellent agreement on the most probable model function, which form is $G(\alpha) = (1 - \alpha)^{-1} - 1$ (integral form) and $f(\alpha) = (1 - \alpha)^2$ (differential form), and its mechanism is chemical reaction. This is verified by the criterion based on activation energy of FWO, and it proves the accuracy and reliability of the analyzed kinetics results.

Acknowledgments

This work is supported by Ph. D. Programs Foundation of Ministry of Education of China (No. 20100042110004) and Fundamental Research Funds for the Central University (No. N090502004 and N140206003).

REFERENCES

[1] X.J. Zheng, Boron Iron Ore Processing, Chemical Industry Press, Beijing (2009).

[2] Q.M. Peng, M.R. Palmer, Econ. Geol. **97**, 93-108 (2002).

[3] X.J. Zheng, Production and Application of Boron Compounds, Chemical Industry Press, Beijing (2008).

[4] Y.F. Lu, Y.C. Cheng, H.Q. Li, C.J. Xue, F.W. Cheng, Acta Geol. Sin. **79**, 408-414 (2005).

[5] Y.Z. Wang, S.J. Liu, Y.G. Jia, R.J. Li, Non-ferrous Mining and Metallurgy **23** (3), 5-8 (2007).

[6] X.J. Fu, J.Q. Zhao, S.Y. Chen, Z.G. Liu, T.L. Guo, M.S. Chu, J. Iron Steel Res. Int. **22** (8), 672-680 (2015).

[7] G. Wang, J.S. Wang, Y.G. Ding, S.Ma, Q.G. Xue, ISIJ Int. **52**, 45-51 (2012).

[8] S.L. Liu, C.M. Cui, X.P. Zhang, ISIJ Int. **38** (10), 1077-1079 (1998).

[9] Z.D. Yang, S.L. Liu, Z.F. Li, X.X. Xue, J. Iron Steel Res. Int. **14** (6), 32-36 (2007).

[10] X.P. Zhang, J.F. Lang, C.M. Cui, S.L. Liu, Iron and Steel, **30** (12), 9-12 (1995).

[11] Y.G. Ding, J.S. Wang, G. Wang, S. Ma, Q.G. Xue, J. Iron Steel Res. Int. **19** (6), 9-13 (2012).

[12] J. Li, Z.G. Fan, Y.L. Liu, S.L. Liu, T. Jiang, Z.P. Xi, Trans. Non-ferrous Met. Soc. China, **20** (6), 1161-1165 (2010).

[13] A. Mergen, M.H. Demirhan, M. Bilene, Adv. Powder Technol. **14** (3), 279-293 (2003).

[14] Z.T. Sui, P.X. Zhang, C. Yamauchi, Acta Mater. **47** (4), 1337-1344 (1999).

[15] P.X. Zhang, Z.T. Sui, Metall. Mater. Trans. B **26** (2), 345-351 (1995).

[16] N. Acarkan, G. Bulut, O. Kangal, G. Onal, Mine. Eng. **18** (7), 739-741 (2005).

[17] G.H. Li, B.J. Liang, M.J. Rao, Y.B. Zhang, T. Jiang, Mine. Eng. **56**, 57-60 (2014).

[18] R.Z. Hu, Thermal Analysis Kinetics[M]. 2nd ed. Science Press, Beijing (2008).

[19] S. Vyazovkin, C.A. Wight, Int. Rev. Phys. Chem. **17** (3), 407-433 (1998).

[20] S. Vyazovkin, Int. Rev. Phys. Chem. **19** (1), 45-60 (2000).

[21] T. Ozawa, Bull. Chem. Soc. Jan. **38** (11), 1881-1886 (1965).

[22] J.H. Flynn, L.A. Wall, J. Polym. Sci. Part B, Polymer Letters. **4** (5), 323-328 (1996).

[23] H.E. Kissinger, Anal. Chem. **29** (11), 1702-1706 (1957).

[24] V. Satava, Thermochim. Acta. **2** (5), 423-428 (1971).

[25] C. Popescu, Thermochim. Acta. **285** (2), 309-323 (1996).

[26] J.J. Zhang, N. Ren, J.H. Bai, Chin. J. Chem. **24** (3), 360-364 (200).